

# SHANGUS: Deep Reinforcement Learning Meets Heuristic Optimization for Speedy Frontier-Based Exploration of Autonomous Vehicles in Unknown Spaces

Seunghyeop Nam, Tuan Anh Nguyen *IEEE Member*, Eunmi Choi, Dugki Min

**Abstract**—This paper introduces SHANGUS, an advanced framework combining Deep Reinforcement Learning (DRL) with heuristic optimization to improve frontier-based exploration efficiency in unknown environments, particularly for intelligent vehicles in autonomous air services, search and rescue operations, and space exploration robotics. SHANGUS harnesses DRL’s adaptability and heuristic prioritization, markedly enhancing exploration efficiency, reducing completion time, and minimizing travel distance. The strategy involves a frontier selection node to identify unexplored areas and a DRL navigation node using the Twin Delayed Deep Deterministic Policy Gradient (TD3) algorithm for robust path planning and dynamic obstacle avoidance. Extensive experiments in ROS2 and Gazebo simulation environments show SHANGUS surpasses representative traditional methods like the Nearest Frontier (NF), Novel Frontier-Based Exploration Algorithm (CFE), and Goal-Driven Autonomous Exploration (GDAE) algorithms, especially in complex scenarios, excelling in completion time, travel distance, and exploration rate. This scalable solution is suitable for real-time autonomous navigation in fields such as industrial automation, autonomous driving, household robotics, and space exploration. Future research will integrate additional sensory inputs and refine heuristic functions to further boost SHANGUS’s efficiency and robustness.

**Index Terms**—Frontier-based Exploration, Deep Reinforcement Learning, Heuristic Optimization, Autonomous Navigation, SLAM

## I. INTRODUCTION

Intelligent vehicles, essential for autonomous airport services [1], search and rescue operations [2, 3], and space exploration [4], exhibit high-level autonomy and can navigate and operate in complex, unknown environments. While current systems perform self-navigation and manipulation given a pre-constructed environment model, some applications necessitate autonomous perception capabilities due to the absence of prior environment models. Leveraging 3D mapping and DRL, these vehicles autonomously navigate and execute tasks, minimizing human intervention and enhancing safety [5]. Existing systems often require partial pre-known environment information for path planning [6, 7], but these frameworks are ineffective in entirely unknown settings. Alternatively, active SLAM strategies without pre-known information [8–10] have limited application due to their non-optimal greedy exploration or poor generalization in complex 3D scenarios. Consequently, a strategy integrating the strengths of these existing methods is needed.

Effective robot integration depends on adapting to environmental data through frontier-based exploration, yet current algorithms are inefficient in exploration and collision avoidance [11]. Recent DRL advancements enable superior, real-time navigation, outperforming traditional methods in dynamic obstacle avoidance [12, 13]. DRL faces challenges in complex environments, prompting research into combining DRL with global path planning and heuristics [14]. Unlike `move_base` or `nav2`, DRL adapts to real-time goals and unexplored spaces, addressing inefficiencies in existing frontier-based exploration strategies.

This work proposes an innovative framework combining DRL and heuristic functions to enhance frontier selection, surpassing existing algorithms. The framework emphasizes efficient exploration beyond visited areas, demonstrating superior performance over traditional methods. It highlights the importance of effective algorithms for initializing and navigating diverse environments. The integration of DRL and heuristic functions redefines indoor robot navigation, achieving remarkable efficiency. The DRL-based frontier selection algorithm assigns weights to distances using a normalized hyperbolic-exponential function. Prioritizing exploration points as closed, open, or step structures, the point with the minimum score (`argmin`) becomes the DRL control goal.

The **key contributions and findings** of this study are as follows:

- **Proposed Speedy Heuristic Approach for Navigating Geographical Unexplored Spaces (SHANGUS):** The SHANGUS framework integrates deep reinforcement learning (DRL) with heuristic optimization to enhance frontier-based exploration efficiency in unknown environments. It leverages DRL’s adaptability and heuristic prioritization, significantly enhancing exploration efficiency, reducing completion time, and travel distance.
- **Novel Frontier Selection and Navigation Strategy:** This strategy includes a frontier selection node for identifying unexplored areas and a DRL navigation node using the Twin Delayed Deep Deterministic Policy Gradient (TD3) algorithm for robust path planning and obstacle avoidance. The heuristic function prioritizes exploration points by considering distance and occupancy stochastic scores, ensuring the selection of valuable, reachable frontiers.
- **Comprehensive Experimental Evaluation and Supe-**

**rior Performance:** Extensive experiments in a ROS2 and Gazebo simulation compare SHANGUS with traditional methods like NF, CFE, and GDAE across varying complexities. SHANGUS significantly outperforms traditional methods in completion time, travel distance, and exploration rate, particularly in complex settings, showcasing adaptability and reliability across various scenarios.

- **Robust and Scalable Solution for Real-Time Navigation:** This solution utilizes DRL and heuristic optimization for efficient real-time navigation in dynamic and unknown spaces. SHANGUS offers a robust, scalable solution for real-time autonomous exploration in diverse applications, including industrial automation, autonomous driving, household robotics, and space exploration vehicles.
- **Extensive Validation and Industrial Relevance:** Extensive simulations validate SHANGUS’s efficiency in environment exploration, representing a significant advancement in robotic navigation, relevant for autonomous driving, industrial mobility, household robotics and space exploration vehicles. Future research will incorporate additional sensory inputs and refine heuristics to further enhance efficiency and robustness.

The remaining is organized as follows. Section II reviews related works on frontier-based exploration, reinforcement learning enhancements, and hybrid approaches. Section III details the SHANGUS framework, including SLAM, DRL-based navigation with TD3, and the frontier exploration algorithm. Section IV presents experimental results comparing SHANGUS to traditional methods across various scenarios. Section V concludes with key findings and future research directions.

## II. RELATED WORKS

Frontier-based exploration strategies are pivotal in autonomous robotics, systematically guiding the exploration of unknown environments by identifying boundaries between explored and unexplored areas. Research spans traditional algorithms to advanced methods integrating machine learning, particularly reinforcement learning (RL).

*a) Traditional Frontier-Based Methods:* Yamauchi [15] laid the foundation for frontier-based exploration, focusing on geometric identification of frontiers [16]. Enhancements include energy-efficient path planning [17], clustering algorithms for frontier management [18], and heuristic optimizations [19].

*b) Reinforcement Learning Enhancements:* Integrating RL into frontier-based exploration allows dynamic adaptation and optimization of exploration strategies. RL-based methods, such as those by Li et al. [20], use deep learning to enhance real-time navigation in complex environments [2], reducing exploration time and increasing coverage efficiency [12].

*c) Hybrid and Advanced Methods:* Hybrid methods combining traditional frontier-based approaches with RL and other machine learning techniques leverage the strengths of both. Cao et al. [13] and Jain et al. [21] merge RL with traditional

metrics for better decision-making. Mackay et al. [22] incorporate dynamic elements to tackle challenges in environments with moving obstacles.

*d) Evaluation and Comparisons:* Evaluations and comparisons of different methods are crucial. Xu et al. [23] provide benchmarks and datasets to assess frontier-based and RL-based exploration strategies, highlighting their performance across diverse scenarios.

*e) Remarks:* Frontier-based exploration is evolving with innovations integrating complex computational models and learning algorithms. Future directions include adaptive learning mechanisms and multi-robot system exploration [24], enhancing collaborative autonomous exploration capabilities.

## III. SHANGUS: SPEEDY HEURISTIC APPROACH FOR NAVIGATING GEOGRAPHICAL UNEXPLORED SPACES

### A. Overall Framework

The SHANGUS framework is designed for autonomous navigation using Gazebo for simulation. It includes several components. The Robot State Publisher, equipped with a LiDAR sensor providing a 360-degree scan array (`Scan(n=360)`) and an odometry sensor tracking position (`Pose: x,y,z`) and orientation (`raw, pitch, yaw`), along with Turtlebot3 Waffle PI’s joint state, supplies vital data. The SLAM Node, using a Bayesian Revision Cycle, generates and updates an occupancy grid map (`Occupancy Grid Map`). The Frontier Selection Node detects unexplored areas, generating point arrays (`Point Arrays`) and uses a heuristic function ( $\mathcal{F} = \{(x,y) \mid \text{given frontier points}\} \rightarrow \min h(f_x, f_y)$ ) for goal selection. The DRL Navigation Node handles local path planning and collision avoidance, using a DRL Control Agent (TD3) for decision-making based on states ( $s, s'$ ), rewards ( $r$ ), and actions ( $a$ ). The Automatic Control Manager manages sensor data, reward calculation, actuation, and acts as a proxy for the DRL agent. Control signals for linear and angular velocity (`Linear velocity, Angular velocity`) are sent to the Turtlebot3, enabling navigation towards goals while avoiding obstacles. This architecture integrates SLAM, frontier-based exploration, and deep reinforcement learning for robust autonomous navigation.

### B. SLAM

SLAM is pivotal in robotics, especially for path planning, a key aspect of this research. SLAM allows a robot to map observed landmarks while probabilistically determining its location. Here, we employ SLAM from the nav2 package in ROS2. **Sensor Data Collection:** Nav2 collects environmental data via LiDAR and cameras, formatted as ROS 2 messages. **Costmap Generation:** This data generates a costmap of the robot’s environment, highlighting navigable areas and obstacles. **Robot Localization using AMCL:** AMCL, a probabilistic algorithm, estimates and updates the robot’s position using sensor data. **Application of SLAM Algorithm:** Nav2 uses SLAM algorithms, like gmapping, to map the environment, enabling simultaneous exploration and localization. **Map Update and Path**

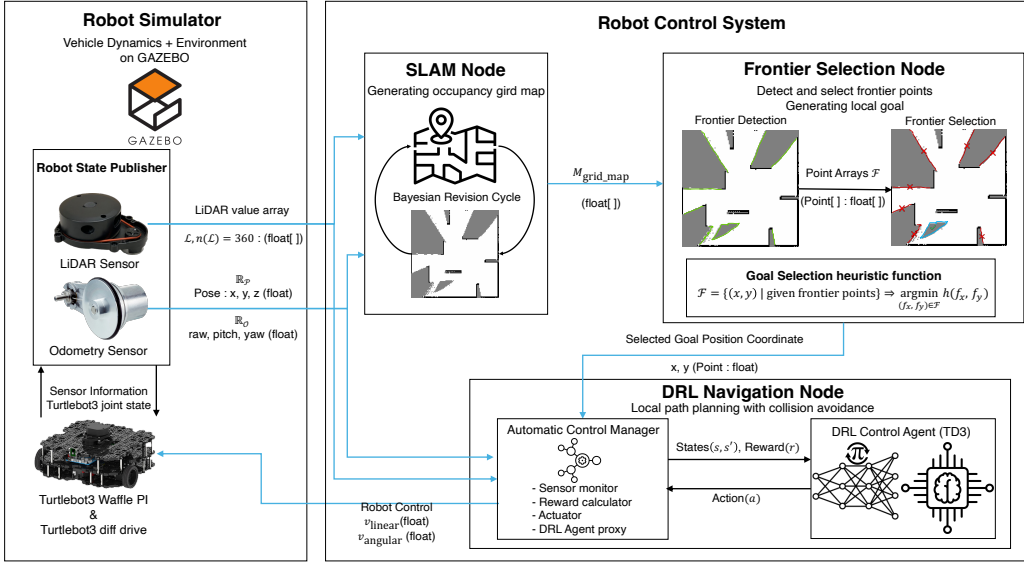


Fig. 1: SHANGUS Framework

**Planning:** The SLAM-generated map is continuously updated for path planning, helping the robot understand and navigate its environment. **Autonomous Navigation:** The robot follows the planned path, adapting to environmental changes detected via sensors. Our proposed algorithm integrates frontier exploration, goal selection, and navigation, enhancing autonomous navigation efficiency.

### C. TD3-based Autonomous Navigation

DRL is instrumental in autonomous robot navigation, learning complex policies from high-dimensional sensor inputs via environmental interactions. Unlike traditional control methods relying on manual features and prior maps, DRL excels in dynamic, unknown environments, crucial for real-time navigation. Algorithms like Proximal Policy Optimization (PPO) and Deep Q-Network (DQN) enhance policy learning stability and efficiency. PPO uses actor-critic networks with residual blocks to improve information flow and mitigate vanishing gradients, accelerating learning. Sensors such as LiDAR and cameras enable environmental comprehension, optimizing decision-making. Simulation environments like ROS and Gazebo facilitate safe, extensive training, with reward functions guiding behaviors like target approach and collision avoidance. Challenges include data inefficiency and generalization, with ongoing research improving sample efficiency and transfer learning for better real-world adaptation [25]. The Twin Delayed Deep Deterministic Policy Gradient (TD3) algorithm, developed by Scott Fujimoto *et al.* [26], is a Policy Gradient method improving upon Deep Deterministic Policy Gradient (DDPG) for high-dimensional continuous action spaces. TD3 addresses value function overestimation in value-based (e.g., DQN) and policy-based (e.g., Actor-Critic) reinforcement learning using Clipped Double Q-learning, Delayed Policy and Target Updates, and Target Policy Smoothing, enhancing stability and performance.

In Clipped Double Q-learning, TD3 uses two independent critic networks to estimate the value function, reducing overes-

timization by taking the minimum value between the two critics, thus enhancing learning stability.

$$\begin{aligned}
 y_1 &= r + \gamma Q_{\theta'_2}(s', \pi_{\phi_1}(s')) \\
 y_2 &= r + \gamma Q_{\theta'_1}(s', \pi_{\phi_2}(s')) \\
 y &= r + \gamma \min(Q_{\theta'_2}(s', \pi_{\phi_1}(s')), Q_{\theta'_1}(s', \pi_{\phi_2}(s')))
 \end{aligned} \tag{1}$$

Here,  $r$  is the reward,  $\gamma$  is the discount factor,  $Q_{\theta'_1}(s', \pi_{\phi_1}(s'))$  and  $Q_{\theta'_2}(s', \pi_{\phi_2}(s'))$  are the Q-values from the critic networks with parameters  $\theta'_1$  and  $\theta'_2$ , and  $\pi_{\phi}(s')$  is the action selected by the policy network at the next state  $s'$ . By taking the minimum of these Q-value predictions, TD3 mitigates overestimation, a common issue in reinforcement learning algorithms.

In Delayed Policy and Target Updates, TD3 updates the policy network (actor) less frequently than the value networks (critics) to ensure the value estimates are more accurate. Typically, the policy network is updated once every two or more updates of the critic networks. This method reduces policy overfitting by averaging Q-values over a range of actions around the target action, thereby improving stability and performance.

$$\theta \leftarrow \tau\theta + (1 - \tau)\theta' \tag{2}$$

where  $\tau$  is the update coefficient.

In the Target Policy Smoothing technique, TD3 adds noise to the target policy during updates to address overfitting and enhance robustness. This approach regularizes value estimation around the target action, mitigating inaccuracies from function approximation errors, and ensuring stable, effective training.

$$\begin{aligned}
 y &= r + \mathbb{E}_{\epsilon \sim \text{clip}(\mathcal{N}(0, \sigma), -c, c)} [Q_{\theta'}(s', \pi_{\phi'}(s') + \epsilon)] \\
 \epsilon &\sim \text{clip}(\mathcal{N}(0, \sigma), -c, c)
 \end{aligned} \tag{3}$$

Applying these three techniques, TD3 enhances performance and stability in reinforcement learning, making it a

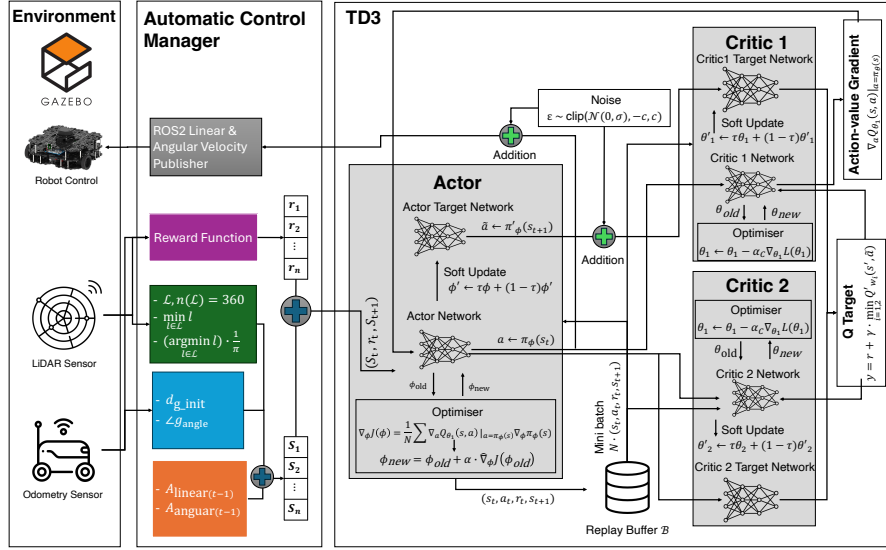


Fig. 2: TD3 based SHANGUS's Autonomous Control

leading algorithm in various environments. The implementation of TD3 is shown in Figure 2, and the actor-critic architecture in Figure 3. Our research employs the TD3 algorithm for vehicle navigation in unknown spaces, relying solely on LiDAR and odometry sensor data, bypassing map dependency. Unlike typical ROS2 nav2 navigation packages, our approach facilitates high-speed navigation during exploration. The automatic control manager node, receiving sensor data from the robot state publisher in the GAZEBO simulation, concatenates this data with previous actions to form states for the actor. It calculates the reward for each action and provides the current state, reward, and next state to the agent. The TD3 actor receives these inputs  $(S_t, r_t, S_{t+1})$  and determines actions within a 2-dimensional action space ( $A_{\text{linear}}$  and  $A_{\text{angular}}$ ). These actions are converted into robot control signals by the automatic control manager node. During training, the critic networks use the same input as the actor network for the first fully connected layer, combining it with the actor-derived action  $a \leftarrow \pi_\phi(s_t)$  for the second layer, producing the  $Q$  value. The training process follows the standard TD3 algorithm.

1) *Reward Design*: The reward function for TD3 in Algorithm 1 integrates factors to guide a robot's exploration in unknown environments. It calculates rewards to ensure the agent avoids obstacles and reaches the goal quickly. Positive rewards are given if the Euclidean distance to the goal ( $d_{g\_robot}$ ) is less than the initial distance ( $d_{g\_init}$ ) or within the goal threshold ( $T_g$ ). Negative rewards (penalties) are applied if the robot fails to maintain maximum linear velocity ( $M_{\text{linear}}$ ), minimum angular action ( $A_{\text{angular}}$ ), or proper orientation ( $\angle g_{\text{angle}}$ ). Penalties also occur if LiDAR values ( $\mathcal{L}$ ) fall below the collision threshold ( $T_c$ ) or  $1.5 \cdot T_c$ .

#### D. Speedy Frontier Exploration and Goal Selection Algorithm

1) *Frontier Detection*: The frontier detection algorithm in Algorithm 2 requires the occupancy grid map  $M$ . It identifies free space ( $\sigma_f$ ), obstacles ( $\sigma_o$ ), and unknown space ( $\sigma_u$ ). The algorithm finds  $\sigma_u$  cells adjacent to  $\sigma_f$  and expands these to

#### Algorithm 1 Reward Function of DRL Algorithm

```

1:  $r_{\text{yaw}} \leftarrow -|\angle g_{\text{angle}}|$ 
2:  $r_{\text{linear}} \leftarrow -((M_{\text{linear}} - A_{\text{linear}}) \cdot 10)^2$ 
3:  $r_{\text{angular}} \leftarrow -A_{\text{angular}}^2$ 
4:  $r_{\text{distance}} \leftarrow \frac{d_{g\_init}}{2 \cdot d_{g\_robot} - 1}$ 
5: if  $\min_{l \in \mathcal{L}} l < 1.5 \cdot T_c$  then
6:    $r_{\text{obstacle}} \leftarrow -50$ 
7: else
8:    $r_{\text{obstacle}} \leftarrow 0$ 
9: end if
10:  $R \leftarrow \sum \{r_{\text{yaw}}, r_{\text{angular}}, r_{\text{distance}}, r_{\text{distance}}, r_{\text{obstacle}}\}$ 
11: if  $d_{g\_robot} < T_g$  then
12:    $R \leftarrow R + 5000$ 
13: end if
14: if  $\min_{l \in \mathcal{L}} l < T_c$  then
15:    $R \leftarrow R - 2000$ 
16: end if
17:
18: return  $R$ 

```

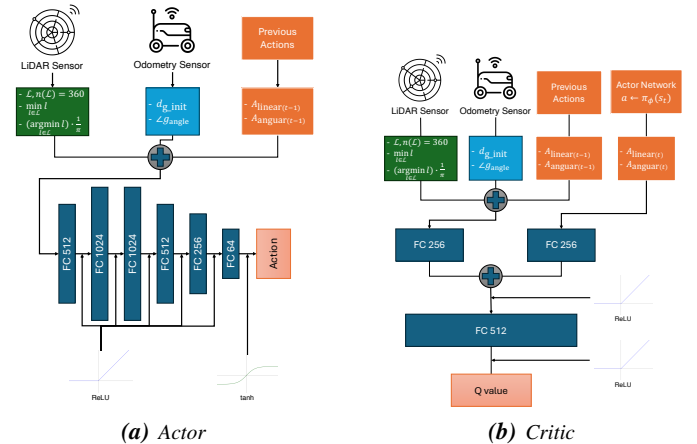


Fig. 3: Actor-Critic Architecture



all 8 directions, marking them as frontier points with value  $f$ . The set of  $f$  cells, representing  $\mathcal{F}$ , is returned as an array.

---

**Algorithm 2** Frontier Detection
 

---

```

1: Initialize  $\mathcal{F}$  as an array with the same dimensions as  $M$ , filled with Non-Frontier marks
2: Set  $w$  and  $h$  as width and height of given map
3: for  $i = 0$  to  $w - 1$  and  $j = 0$  to  $h - 1$  do
4:   if  $M[i + w \cdot j]$  is  $\sigma_f$  then
5:     if  $i > 0$  and  $M[(i - 1) + w \cdot j]$  is  $\sigma_o$  then
6:        $\mathcal{F}[i + w \cdot j] \leftarrow f$ 
7:     else if  $i < w - 1$  and  $M[(i + 1) + w \cdot j]$  is  $\sigma_u$  then
8:        $\mathcal{F}[i + w \cdot j] \leftarrow f$ 
9:     else if  $j > 0$  and  $M[i + w \cdot (j - 1)]$  is  $\sigma_u$  then
10:       $\mathcal{F}[i + w \cdot j] \leftarrow f$ 
11:    else if  $j < h - 1$  and  $M[i + w \cdot (j + 1)]$  is  $\sigma_u$  then
12:       $\mathcal{F}[i + w \cdot j] \leftarrow f$ 
13:    end if
14:  end if
15: end for
16:
17: return  $F_{\text{mask}}$ 

```

---

2) *Occupancy Stochastic Score*: The Occupancy Stochastic Score, as the name suggests, involves analyzing the occupancy grid map of the area where the frontier is located to calculate how worthwhile it is to explore that region. The score is computed as in the Equation 4:

$$O(f_x, f_y) = \frac{\sum_{(x,y) \in S} m(x,y)}{\pi r^2} \quad (4)$$

where  $(c_x, c_y)$  is coordinate of frontier centroid point.  $m(x,y)$  is occupancy value on coordinate on  $(x,y)$   $S := \{(x,y) \mid (x - f_x)^2 + (y - f_y)^2 \leq r^2\}$

This function  $m(x,y)$  represents the occupancy value score at point  $(x,y)$  on the map. According to the `costmap2D` package in ROS2, inflation propagates cost values from occupied cells, decreasing with distance. We define 5 specific symbols for costmap values related to the robot:

- "Lethal" cost indicates an actual obstacle in a cell, implying collision if the robot's center is there.
- "Inscribed" cost means a cell is within the robot's inscribed radius from an obstacle, ensuring collision if the robot's center is there.
- "Possibly circumscribed" cost, using the robot's circumscribed radius, implies potential collision depending on the robot's orientation. This value may also represent user-defined costs to avoid specific areas.
- "Freespace" cost, assumed to be zero, means no obstacles are present.
- "Unknown" cost signifies no information about a cell, open to user interpretation.

Other costs range between "Freespace" and "Possibly circumscribed" based on their distance from a "Lethal" cell and a user-defined decay function. This flexibility allows planners to account for footprint only when orientation matters. Each cell on the map has 255 stochastic values. Remapping the value 255 (unknown space) to 0 and adding 1 to the remaining values sets unknown space to 0, while known space with higher obstacle likelihood gets higher values. Cells certain to have obstacles (probability 1)

get the maximum value of 255, indicating exploration value. To determine exploration value, we set the radius  $r$  from the frontier centroid to the farthest frontier cell. Summing the probability values of cells within a circle centered at the frontier centroid and dividing by the circle's area gives the average probability value, ranging  $[0, 1]$ . Values near 0 indicate dominant unknown space or many free spaces, while values near 1 indicate primarily obstacle-occupied space, thus lower exploration value.

3) *Frontier Types*: Exploration areas can be categorized into three types based on the map formation.

a) *Closed Frontier*: Closed frontiers typically occur between explored areas, appearing as unexplored gaps. Prioritizing these areas enhances efficiency, preventing the need for the robot to return later. Characteristics include a red boundary indicating the frontier line, a green centroid, a yellow farthest point from the centroid, and a blue circle with the radius equal to the yellow line. The unknown space within the circle dominates, yielding an occupancy stochastic score close to 0, the lowest among the three types.

b) *Open Wide Frontier*: Open wide frontiers arise in large open spaces detected by the robot's lidar sensor, where beyond the sensor's threshold remains unknown. Prioritizing these frontiers leads to efficient exploration as they align with the robot's exploration direction. The occupancy stochastic score here is higher than in closed frontiers due to a mix of unknown space, free space, and some obstacles, making it the second priority.

c) *Door Gap Frontier*: Door gap frontiers occur in gaps between obstacles, such as open doors. These frontiers appear when transitioning between spaces or changing paths. To ensure efficiency, this type should be the lowest priority if the current area isn't fully explored. The occupancy stochastic score indicates a higher proportion of free space with some unknown areas, resulting in the highest score among the three types, making it the last choice for exploration.

4) *Speedy Heuristic Function*: A heuristic function (Equation 5) uses empirical knowledge to solve problems efficiently by reducing search paths and time, thus improving speed and effectiveness in finding optimal solutions. For short distances, the score converges to 0, ensuring no difference between scores. Beyond a threshold, the derivative increases rapidly then decreases, converging to  $\gamma$ , excluding these distances. The distance score is divided into three sections: close-range, proportional range, and far-range.

Normalizing regional probability characteristics with  $\frac{1}{\cosh a_f}$ , where  $a_f$  is the frontier length, and multiplying by the frontier length, calculates the occupancy stochastic score considering openness and size. Combining the distance score and occupancy stochastic score yields the final heuristic function (Equation 5).

$$\begin{aligned}
h(f_i) &= \text{Score}(f_x, f_y) \\
&= \tanh \left( e^{\frac{d(f_x, f_y)}{\beta}} \cdot \sigma \left( e^{\frac{d(f_x, f_y)}{\beta}} \cdot \left( 1 - \text{csch} \frac{d(f_x, f_y)}{\alpha} \right) \right) \right) \cdot \gamma \\
&\quad + (O(f_x, f_y) \cdot \text{sech } a_f) \cdot (1 - \gamma)
\end{aligned} \quad (5)$$

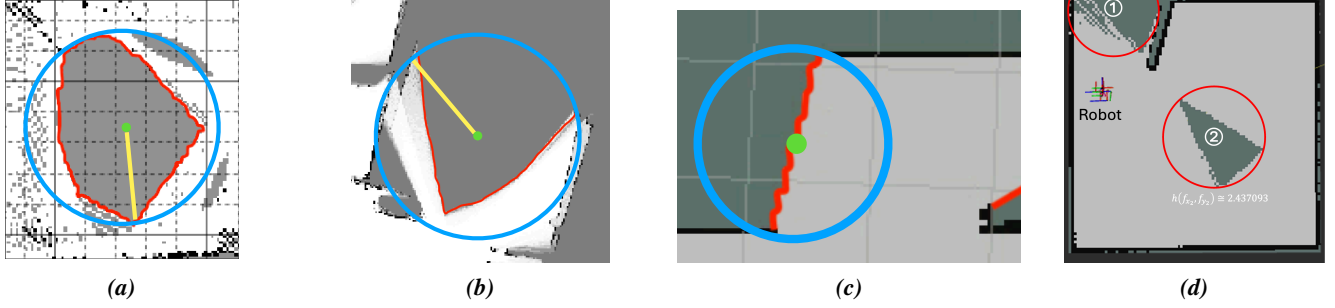


**Fig. 4: Representative Frontiers**  
 (a). Closed Frontier, (b). Open Wided Frontiers, (c). Door Gap Frontier, (d) Case-study

In this formula,  $R$  represents the map resolution, determining the granularity of the occupancy grid map. The term  $a_f$  denotes the frontier's size, indicating its length. The occupancy stochastic score,  $O(f_x, f_y)$ , is calculated as  $O(f_x, f_y) = \frac{\sum_{(x,y) \in S} m(x,y)}{\pi r^2}$ , evaluating a region's worth based on the occupancy values within a circle of radius  $r$  centered at the frontier point  $(f_x, f_y)$ . Parameters  $\alpha, \beta, \gamma, \delta$  are discount factors modulating the heuristic function, with  $\gamma \leq \delta$ . The robot's position is  $(r_x, r_y)$ . The normalized map value at  $(x, y)$ ,  $m(x, y)$ , is defined as  $m(x, y) = \frac{C(x,y)}{255}$ , where  $C(x, y)$  is the costmap value at  $(x, y)$ . The sigmoid function  $\sigma(x)$  is  $\sigma(x) = \frac{1}{1+e^{-x}}$ . Set  $S$  includes points within a circle centered at  $(f_x, f_y)$  with radius  $r$ ,  $S \equiv \{(x, y) \mid (x - f_x)^2 + (y - f_y)^2 \leq r^2\}$ . The Euclidean distance between  $(r_x, r_y)$  and  $(f_x, f_y)$  is  $d = \sqrt{(r_x - f_x)^2 + (r_y - f_y)^2}$ . The heuristic function combines distance-based and occupancy-based scores to determine a frontier point's overall heuristic value. The distance-based component uses an exponential and hyperbolic cosecant function modulated by discount factors  $\alpha$  and  $\beta$ , followed by a hyperbolic tangent function scaled by  $\gamma$ . The occupancy-based component involves  $O(f_x, f_y)$  scaled by the hyperbolic secant of  $a_f$  and discount factor  $\delta$ . The final frontier goal is selected as the point minimizing this heuristic score,  $\text{Frontier Goal} = \text{argmin}(h(f_i))$ , integrating distance and occupancy information to prioritize valuable frontier points for exploration. As seen in Figure 4d, there are two frontiers, Frontier 1 and Frontier 2. Frontier 1, located between an open area and a door gap, requires more exploration beyond it. Methods like NF, focusing solely on proximity, would initially explore Frontier 1 and later return to Frontier 2. SHANGUS, however, prioritizes Frontier 2 due to its lower heuristic score. The enclosed shape of Frontier 2, with a higher ratio of unknown space and longer frontier length, results in a lower score using the hyperbolic cosine ( $\text{csch}$ ). Thus, SHANGUS favors Frontier 2, avoiding redundant exploration. GDAE, similar in purpose, uses a fixed kernel size for evaluation, which poses generalization challenges, unlike SHANGUS, which adapts the inscribing circle radius for more accurate heuristic calculation.

## IV. EXPERIMENTAL SIMULATION AND RESULTS

### A. Simulation Setup

In an environment implemented with ROS2 and Gazebo Classic, we conducted comparative experiments using the Turtlebot3 waffle\_pi to evaluate each algorithm. The DRL algorithm for local navigation was implemented using TD3, and a Gazebo world with six dynamic obstacles was created. Training was conducted over 10,000 episodes on a system with an Intel(R) Core(TM) i5-10400F CPU @ 2.90GHz and an NVIDIA 3070 GPU, taking approximately two days. Frontier detection and selection were managed by a separate node subscribing to the occupancy grid map via DDS communication, publishing the local goal to the DRL navigation node. Figure 5a illustrates a Gazebo training environment for robot exploration in unknown spaces. Enclosed by a wooden-framed boundary, the grid-based floor is populated with static obstacles (brown boxes, triangular frame, "L" shaped barrier) and dynamic obstacles (white cylindrical pillars). A central robot, equipped with sensors and depicted with a blue radial projection representing its field of view, navigates efficiently around obstacles. A red object near the bottom-left may represent a marker or another robot. This setup simulates a challenging scenario for training in navigation, obstacle avoidance, and spatial awareness.

Figure 5b, Simple Room with Obstacles: Scenario I (Low Complexity Map) features a robot in a small room with internal walls creating separate sections. Blue shaded areas represent the regions scanned by the robot's sensors, indicating its line of sight. The robot's central position and its mapping effort highlight its ability to navigate and identify obstacles and free space in simple environments. Figure 5c, Corridor with Turns: Scenario II (Medium Complexity Map) depicts a corridor with several turns and junctions. The robot's sensors, shown as blue fan-shaped areas, test its navigation through complex paths and tight turns, typical in indoor settings such as office buildings or hospitals. Figure 5d, Complex Maze: Scenario III (High Complexity Map) presents a maze-like environment with multiple rooms and narrow passages. The robot uses its sensors to explore and map this intricate space, challenging its advanced navigation algorithms and

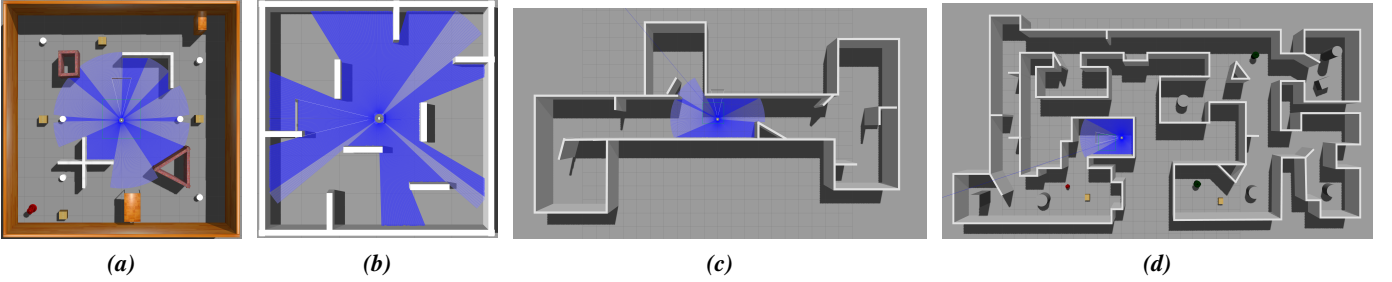


Fig. 5: Simulation Scenarios. (a) Training Environment; (b) Small Space with Obstacles; (b) Corridor with Turns; (c) Complex Maze

TABLE I: Experimental Results in Completing Environment Exploration

Metrics	NF			CFE			GDAE			SHANGUS w/o DRL			SHANGUS w/ DRL		
	I	II	III	I	II	III	I	II	III	I	II	III	I	II	III
Avg dist.(m)	15.471	83.897	210.731	22.162	91.692	268.330	16.958	78.611	211.397	13.151	69.480	163.879	16.655	76.745	175.768
Min dist.(m)	13.027	71.441	180.311	19.357	80.325	210.376	13.806	68.933	187.847	12.170	61.677	153.073	16.655	67.926	161.479
Max dist.(m)	17.540	95.460	244.956	25.998	104.449	337.185	20.388	91.310	267.180	13.985	80.995	188.797	20.531	87.555	194.186
$\sigma$ (dist)	1.840	8.057	21.329	2.418	7.630	31.981	2.039	8.161	23.593	0.667	5.280	10.566	2.717	7.150	12.324
Avg T.(sec)	135.270	542.690	2610.870	123.060	545.520	1552.860	153.470	880.590	1251.900	71.200	352.700	889.190	81.280	325.090	785.340
Min T.(sec)	111.900	487.100	1115.100	109.400	490.200	1277.800	107.900	354.800	1051.600	58.600	310.100	804.100	66.100	276.700	683.100
Max T.(sec)	151.400	670.200	14167.100	140.500	588.100	1764.900	253.600	4545.000	1600.300	86.100	409.200	1019.400	99.700	382.200	870.000
$\sigma$ (T)	13.887	53.853	4063.987	12.147	37.931	167.475	39.445	1290.434	163.315	10.469	30.809	77.790	11.924	37.995	63.175
Avg ExpR.(%)	98.370	99.485	99.099	98.688	99.423	98.981	98.247	99.495	98.971	97.784	99.240	99.557	98.025	99.466	99.735
Min ExpR.(%)	97.501	99.165	95.272	98.261	99.230	95.249	98.010	99.112	97.116	97.486	97.478	99.236	96.453	99.042	99.539
Max ExpR.(%)	99.134	99.866	99.894	99.947	99.697	99.971	98.709	99.738	99.972	98.041	99.996	99.956	99.719	99.880	99.988
$\sigma$ (ExpR)	0.502	0.244	1.463	0.594	0.134	1.944	0.176	0.189	1.128	0.002	0.670	0.190	0.882	0.260	0.123

decision-making for effective exploration and mapping. To evaluate the heuristic function and DRL navigation, we compare our approach with CFE [18], GDAE [14], and NF [15]. CFE uses ROS2's `move_base` for frontier selection based on factors like cluster size and proximity. GDAE, using TD3, adapts for frontier-based exploration with dynamic path updates. The NF algorithm, foundational for frontier-based exploration, guides the robot to the nearest frontier using evidence grids.

## B. Experimental Simulation Results and Analyses

1) *Environment Reveal*: The table I presents a comparative analysis of various autonomous exploration algorithms under three different scenarios. Metrics used for comparison include average distance (Avg dist.), minimum distance (Min dist.), maximum distance (Max dist.), standard deviation of distance ( $\sigma$ (dist)), average time (Avg T.), minimum time (Min T.), maximum time (Max T.), standard deviation of time ( $\sigma$ (T)), average exploration rate (Avg ExpR.), minimum exploration rate (Min ExpR.), maximum exploration rate (Max ExpR.), and the standard deviation of exploration rate ( $\sigma$ (ExpR)). Algorithms compared are NF, CFE, GDAE, SHANGUS without Deep Reinforcement Learning (w/o DRL), and SHANGUS with Deep Reinforcement Learning (w/ DRL).

a) *Scenario I (Low Complexity Map)*:: SHANGUS w/o DRL shows the best performance with the shortest average distance (13.15 meters) and fastest completion time (71.2 seconds). It also has the lowest standard deviation in travel distance (0.67 meters), indicating high consistency. SHANGUS w/ DRL has slightly higher values (16.66 meters and 81.28 seconds) but maintains a high exploration rate (98.03%). NF and CFE achieve high exploration rates (98.37% and 98.69%) but with significantly higher distances and times: NF

(15.47 meters, 135.27 seconds) and CFE (22.16 meters, 123.06 seconds). GDAE has the longest completion time (153.47 seconds) and higher average distance (16.96 meters), despite a high exploration rate (98.25%).

b) *Scenario II (Medium Complexity Map)*:: SHANGUS w/ DRL outperforms others with the shortest average completion time (325.09 seconds) and a high exploration rate (99.47%). Its average distance (76.75 meters) is slightly longer than SHANGUS w/o DRL (69.48 meters) but shows excellent efficiency. SHANGUS w/o DRL also performs well (352.70 seconds, 99.24%). NF and CFE have much longer completion times: NF (542.69 seconds) and CFE (545.52 seconds). GDAE struggles with high variability, averaging 880.59 seconds and 78.61 meters, despite a high exploration rate (99.49%).

c) *Scenario III (High Complexity Map)*:: SHANGUS w/ DRL excels with the shortest average completion time (785.34 seconds) and highest exploration rate (99.74%). Its average distance (175.77 meters) is significantly shorter than NF and CFE. SHANGUS w/o DRL also performs well (889.19 seconds, 99.56%). NF and CFE have much higher times and distances: NF (2610.87 seconds, 210.73 meters) and CFE (1552.86 seconds, 268.33 meters). GDAE, with a lower average distance (211.40 meters), has a very high and variable completion time (1251.90 seconds). This analysis shows SHANGUS w/ DRL and w/o DRL significantly outperform others in complex environments.

2) *Distance by time*: The figures 6a, 6b, and 6c illustrate the performance of GDAE, NF, CFE, SHANGUS w/ DRL, and SHANGUS w/o DRL, shown by different colored lines for robot exploration in unknown spaces (Scenarios I, II, and III). These are evaluated by distance traveled (meters) versus time (seconds). Shaded areas around each line indicate variance, reflecting consistency and reliability. In Scenario

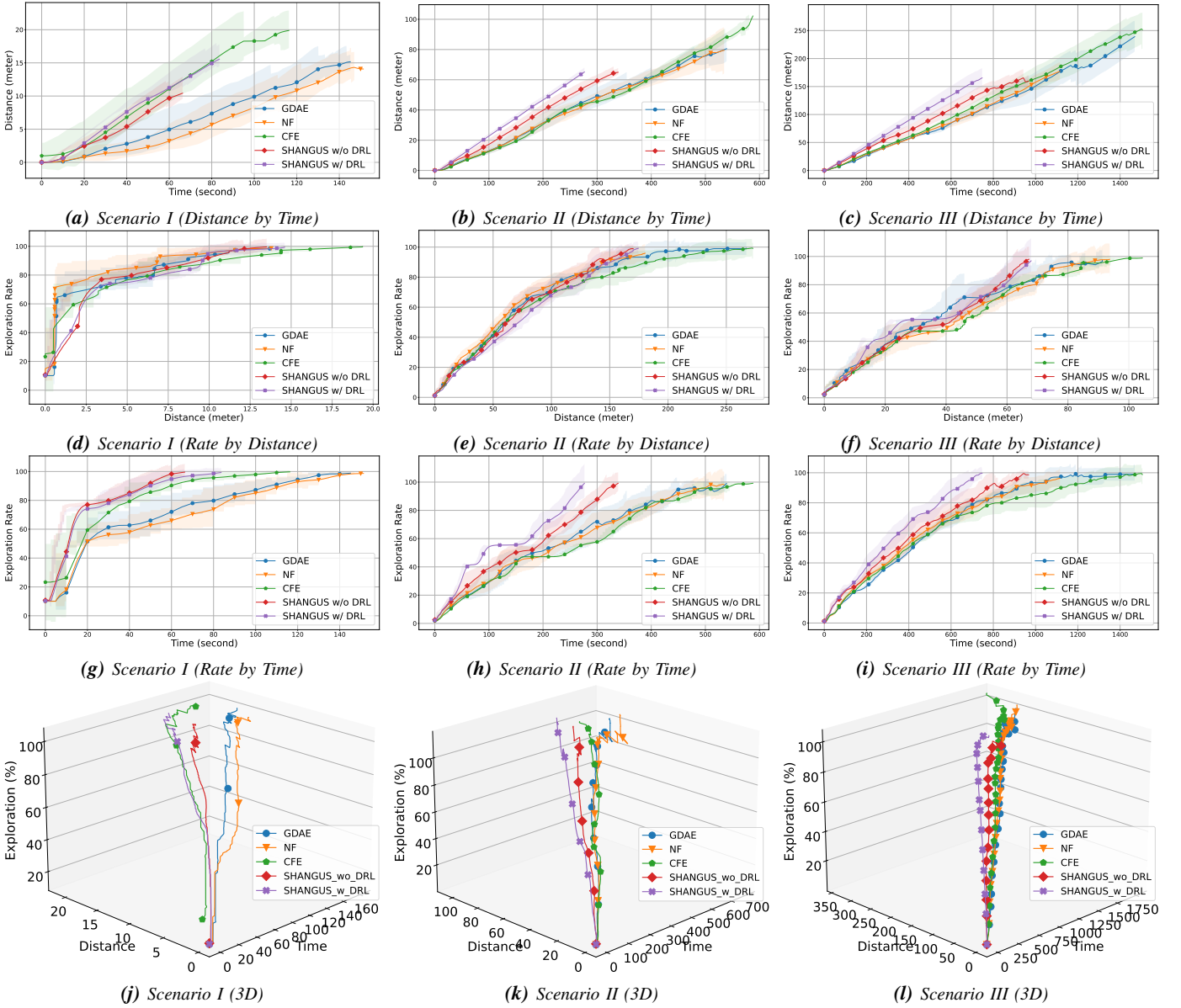


**Fig. 6:** Experimental Simulation Results of Robot Exploration in Unknown Spaces

I (simple complexity), SHANGUS w/ DRL outperforms all algorithms with the shortest travel distances and completion times, followed by SHANGUS w/o DRL. CFE shows intermediate performance, while GDAE and NF are less efficient, with NF being the least effective. As complexity increases in Scenario II (medium complexity) and Scenario III (high complexity), SHANGUS w/ DRL remains the leader, demonstrating improved efficiency and shorter completion times. SHANGUS w/o DRL holds second place, showing slightly increased distances and times. CFE performs reasonably well but lags behind SHANGUS, while GDAE and NF exhibit significantly longer distances and times, with NF consistently the worst performer. Our algorithms, SHANGUS w/o DRL and SHANGUS w/ DRL, increasingly outperform others as complexity rises, particularly SHANGUS w/ DRL, which completes tasks faster. Notably, these algorithms cover more distance within the same travel time under higher complexity,

indicating an effective strategy to explore the map efficiently.

3) *Exploration rate by traversed distance:* Figures 6d, 6e, and 6f illustrate exploration rate (%) versus traversed distance (meters). In Scenario I (simple map), the NF algorithm achieves the highest exploration rates with the shortest distances. In Scenario II (medium complexity), SHANGUS algorithms (w/ and w/o DRL) improve significantly, matching and surpassing other algorithms. In Scenario III (high complexity), SHANGUS w/ DRL exhibits the highest efficiency, achieving the best exploration rates with the shortest distances, followed by SHANGUS w/o DRL. CFE, GDAE, and NF show lower performance levels. Overall, SHANGUS algorithms, especially with DRL, excel in complex exploration tasks, proving the most effective for unknown and intricate spaces.

4) *Exploration rate by traversed time:* The provided graphs show performance in exploration rate over time for GDAE, NF, CFE, SHANGUS w/o DRL, and SHANGUS w/ DRL across



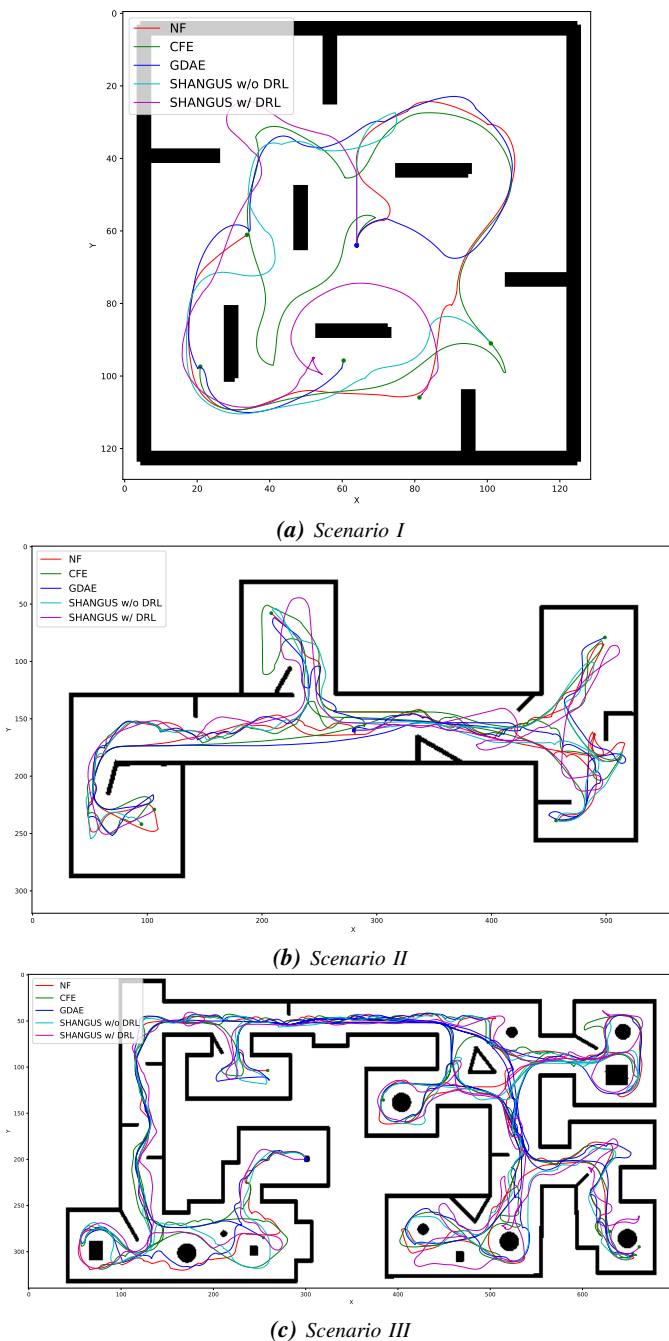


Fig. 7: Exploration paths

three scenarios. In World 01 (0-140 seconds), SHANGUS w/ DRL reaches nearly 80% within 20 seconds and close to 100% by 100 seconds, followed by SHANGUS w/o DRL. CFE steadily increases, while NF and GDAE lag significantly. In World 02 (0-600 seconds), SHANGUS w/ DRL leads again, achieving 80% within 200 seconds and nearing 100% by 500 seconds. SHANGUS w/o DRL reaches 90% by 600 seconds. CFE shows moderate performance, with NF and GDAE under 60%. In World 03 (0-1400 seconds), SHANGUS w/ DRL reaches 80% by 600 seconds and 100% by 1200 seconds, followed by SHANGUS w/o DRL. CFE reaches about 80%, while NF and GDAE remain under 60%. SHANGUS w/ DRL

consistently demonstrates the highest exploration rates, making it the most efficient algorithm, followed by SHANGUS w/o DRL. CFE shows moderate performance, with NF and GDAE being less effective. DRL integration in SHANGUS significantly improves exploration efficiency in unknown environments.

5) *Exploration rate by traversed distance and time:* Figures 6j, 6k, and 6l use 3D plots to illustrate the relationship between exploration rate, traversed distance, and time. If graphs move left, algorithms traverse longer distances in less time. If right, more time is taken with shorter distances. In Scenario I (simple map), SHANGUS w/ DRL and w/o DRL show faster completion compared to GDAE, NF, and CFE. They initially cover more distance but quickly achieve 100% exploration, indicating high efficiency. In Scenario II (medium complexity), SHANGUS algorithms maintain a high exploration rate from the early stages, while other algorithms increase gradually. SHANGUS w/ DRL and w/o DRL optimize traversed distance to achieve exploration objectives swiftly. In Scenario III (high complexity), SHANGUS algorithms continue to excel, completing exploration faster and more efficiently than GDAE, NF, and CFE. Despite longer traversed distances, SHANGUS algorithms complete exploration significantly quicker, showcasing their navigation effectiveness in complex spaces.

6) *Traversed paths:* Figure 7 demonstrates robot paths in three maps of differing complexity: 7a (simple map), 7b (moderate map), and 7c (highly complex map). SHANGUS w/ DRL (magenta) shows the highest efficiency, learning and optimizing behavior to avoid redundant paths. SHANGUS w/o DRL (cyan) performs well but lacks optimization, resulting in some redundant paths. NF (red) and CFE (green) have many redundancies, while GDAE (blue) outperforms NF and CFE but is still behind SHANGUS. In more complex maps, SHANGUS w/ DRL maintains efficiency with minimal retracing and optimal coverage, followed by SHANGUS w/o DRL. GDAE performs reasonably but is surpassed by SHANGUS, while NF and CFE are the least efficient. SHANGUS w/ DRL is the most effective for exploring unknown maps, followed by SHANGUS w/o DRL, GDAE, NF, and CFE.

7) *Discussions:* Results show SHANGUS w/o DRL achieves the shortest average distances, indicating efficient path selection. SHANGUS w/ DRL achieves the lowest average times, suggesting faster exploration. Both SHANGUS variants demonstrate high, consistent exploration rates, with SHANGUS w/o DRL showing lower variability. The SHANGUS framework, both w/ and w/o DRL, enhances exploration efficiency in unknown environments. The heuristic optimization and DRL combination in SHANGUS w/ DRL stands out for speed and reliability, making it a promising approach for autonomous exploration. SHANGUS algorithms outperform others because current algorithms use ROS-based navigation with discrete movements, leading to lower speeds and redundant paths. SHANGUS uses heuristic functions for optimal frontier selection and DRL for fast, continuous navigation, maximizing map revelation in minimal time.

## V. CONCLUSION

Our research demonstrates that the SHANGUS framework, incorporating both heuristic optimization and deep reinforcement learning (DRL), significantly enhances exploration efficiency in unknown environments. Experimental results across three scenarios of varying complexity validate the superiority of SHANGUS algorithms, especially when integrated with DRL. The SHANGUS w/ DRL algorithm consistently achieved the highest exploration rates and shortest completion times, outperforming other traditional and advanced frontier-based exploration methods. These findings underscore the potential of combining heuristic methods with DRL to optimize autonomous navigation, making SHANGUS a promising solution for real-time applications in diverse robotic exploration tasks. Future work will focus on further refining the heuristic functions and integrating additional sensory inputs to enhance robustness and adaptability in more complex and dynamic environments.

## ACKNOWLEDGMENT

This research was partially supported by Basic Science Research Program through the National Research Foundation of Korea(NRF) funded by the Ministry of Education(No. 2020R1A6A1A03046811). This research was supported by Basic Science Research Program through the National Research Foundation of Korea(NRF) funded by the Ministry of Education(2021R1A2C2094943)

## REFERENCES

- [1] Z. Sun *et al.*, “Multi-Risk-RRT: An Efficient Motion Planning Algorithm for Robotic Autonomous Luggage Trolley Collection at Airports,” *IEEE Transactions on Intelligent Vehicles*, vol. 9, no. 2, pp. 3450–3463, 2024, ISSN: 2379-8904. DOI: 10.1109/TIV.2023.3349171 (cit. on p. 1).
- [2] F. Niroui, K. Zhang, Z. Kashino, and G. Nejat, “Deep Reinforcement Learning Robot for Search and Rescue Applications: Exploration in Unknown Cluttered Environments,” *IEEE Robotics and Automation Letters*, vol. 4, no. 2, pp. 610–617, 2019. DOI: 10.1109/LRA.2019.2891991 (cit. on pp. 1–2).
- [3] A. Al-Kaff, F. M. Moreno, A. de la Escalera, and J. M. Armingol, “Intelligent vehicle for search, rescue and transportation purposes,” in *2017 IEEE International Symposium on Safety, Security and Rescue Robotics (SSRR)*, IEEE, 2017, pp. 110–115, ISBN: 978-1-5386-3923-8. DOI: 10.1109/SSRR.2017.8088148 (cit. on p. 1).
- [4] J. Fan, X. Zhang, and Y. Zou, “Hierarchical path planner for unknown space exploration using reinforcement learning-based intelligent frontier selection,” *Expert Systems with Applications*, vol. 230, p. 120630, 2023, ISSN: 0957-4174. DOI: <https://doi.org/10.1016/j.eswa.2023.120630> (cit. on p. 1).
- [5] Y. Xue and W. Chen, “Multi-Agent Deep Reinforcement Learning for UAVs Navigation in Unknown Complex Environment,” *IEEE Transactions on Intelligent Vehicles*, vol. 9, no. 1, pp. 2290–2303, 2024, ISSN: 2379-8904. DOI: 10.1109/TIV.2023.3298292 (cit. on p. 1).
- [6] S. Achat, Q. Serdel, J. Marzat, and J. Moras, “A Case Study of Semantic Mapping and Planning for Autonomous Robot Navigation,” *SN Computer Science*, vol. 5, no. 1, p. 55, 2023, ISSN: 2661-8907. DOI: 10.1007/s42979-023-02370-3 (cit. on p. 1).
- [7] R. Zhang *et al.*, “Efficient and Near-Optimal Global Path Planning for AGVs: A DNN-Based Double Closed-Loop Approach With Guarantee Mechanism,” *IEEE Transactions on Industrial Electronics*, pp. 1–12, 2024. DOI: 10.1109/TIE.2024.3409883 (cit. on p. 1).
- [8] W. Zhao, Q. Meng, and P. W. H. Chung, “A Heuristic Distributed Task Allocation Method for Multivehicle Multitask Problems and Its Application to Search and Rescue Scenario,” *IEEE Transactions on Cybernetics*, vol. 46, no. 4, pp. 902–915, 2016. DOI: 10.1109/TCYB.2015.2418052 (cit. on p. 1).
- [9] J. Chen, K. Wu, M. Hu, P. N. Suganthan, and A. Makur, “LiDAR-Based End-to-End Active SLAM Using Deep Reinforcement Learning in Large-Scale Environments,” *IEEE Transactions on Vehicular Technology*, pp. 1–14, 2024. DOI: 10.1109/TVT.2024.3405483 (cit. on p. 1).
- [10] Y. Yin, Z. Chen, G. Liu, J. Yin, and J. Guo, “Autonomous navigation of mobile robots in unknown environments using off-policy reinforcement learning with curriculum learning,” *Expert Systems with Applications*, vol. 247, p. 123202, 2024, ISSN: 0957-4174. DOI: <https://doi.org/10.1016/j.eswa.2024.123202> (cit. on p. 1).
- [11] M. Keidar and G. A. Kaminka, “Robot exploration with fast frontier detection: theory and experiments,” in *Proceedings of the 11th International Conference on Autonomous Agents and Multiagent Systems - Volume 1*, ser. AAMAS '12, Richland, SC: International Foundation for Autonomous Agents and Multiagent Systems, 2012, pp. 113–120, ISBN: 0981738117 (cit. on p. 1).
- [12] A. Peake, J. McCalmon, Y. Zhang, D. Myers, S. Alqah-tani, and P. Pauca, “Deep Reinforcement Learning for Adaptive Exploration of Unknown Environments,” in *2021 International Conference on Unmanned Aircraft Systems (ICUAS)*, 2021, pp. 265–274. DOI: 10.1109/ICUAS51884.2021.9476756 (cit. on pp. 1–2).
- [13] Y. Cao, R. Zhao, Y. Wang, B. Xiang, and G. Sartoretto, “Deep Reinforcement Learning-Based Large-Scale Robot Exploration,” *IEEE Robotics and Automation Letters*, vol. 9, no. 5, pp. 4631–4638, 2024. DOI: 10.1109/LRA.2024.3379804 (cit. on pp. 1–2).
- [14] R. Cimurs, I. H. Suh, and J. H. Lee, “Goal-Driven Autonomous Exploration Through Deep Reinforcement Learning,” *IEEE Robotics and Automation Letters*, vol. 7, no. 2, pp. 730–737, 2022. DOI: 10.1109/LRA.2021.3133591 (cit. on pp. 1, 7).



- [15] B Yamauchi, “A frontier-based approach for autonomous exploration,” in *Proceedings 1997 IEEE International Symposium on Computational Intelligence in Robotics and Automation CIRA'97. 'Towards New Computational Principles for Robotics and Automation'*, 1997, pp. 146–151. DOI: 10.1109/CIRA.1997.613851 (cit. on pp. 2, 7).
- [16] D. Holz, N. Basilico, F. Amigoni, and S. Behnke, “Evaluating the Efficiency of Frontier-based Exploration Strategies,” in *ISR 2010 (41st International Symposium on Robotics) and ROBOTIK 2010 (6th German Conference on Robotics)*, 2010, pp. 1–8 (cit. on p. 2).
- [17] Y. Mei, Y.-H. Lu, C. S. G. Lee, and Y. C. Hu, “Energy-efficient mobile robot exploration,” in *Proceedings 2006 IEEE International Conference on Robotics and Automation, 2006. ICRA 2006.*, 2006, pp. 505–511. DOI: 10.1109/ROBOT.2006.1641761 (cit. on p. 2).
- [18] D. L. da Silva Lubanco, M. Pichler-Scheder, and T. Schlechter, “A Novel Frontier-Based Exploration Algorithm for Mobile Robots,” in *2020 6th International Conference on Mechatronics and Robotics Engineering (ICMRE)*, 2020, pp. 1–5. DOI: 10.1109/ICMRE49073.2020.9064866 (cit. on pp. 2, 7).
- [19] R. Cimurs, I. H. Suh, and J. H. Lee, “Information-Based Heuristics for Learned Goal-Driven Exploration and Mapping,” in *2021 18th International Conference on Ubiquitous Robots (UR)*, 2021, pp. 571–578. DOI: 10.1109/UR52253.2021.9494668 (cit. on p. 2).
- [20] Z. Li, J. Xin, and N. Li, “Autonomous Exploration and Mapping for Mobile Robots via Cumulative Curriculum Reinforcement Learning,” in *2023 IEEE/RSJ International Conference on Intelligent Robots and Systems (IROS)*, IEEE, 2023, pp. 7495–7500, ISBN: 978-1-6654-9190-7. DOI: 10.1109/IROS55552.2023.10342066 (cit. on p. 2).
- [21] U. Jain, R. Tiwari, and W. W. Godfrey, “Comparative study of frontier based exploration methods,” in *2017 Conference on Information and Communication Technology (CICT)*, 2017, pp. 1–5. DOI: 10.1109/INFOCOMTECH.2017.8340589 (cit. on p. 2).
- [22] A. K. Mackay, L. Riazuelo, and L. Montano, “RL-DOVS: Reinforcement Learning for Autonomous Robot Navigation in Dynamic Environments,” *Sensors*, vol. 22, no. 10, 2022, ISSN: 1424-8220. DOI: 10.3390/s22103847 (cit. on p. 2).
- [23] Y. Xu *et al.*, “Explore-Bench: Data Sets, Metrics and Evaluations for Frontier-based and Deep-reinforcement-learning-based Autonomous Exploration,” in *2022 International Conference on Robotics and Automation (ICRA)*, 2022, pp. 6225–6231. DOI: 10.1109/ICRA46639.2022.9812344 (cit. on p. 2).
- [24] J. Vaščák and D. Herich, “Map Merging for Multi-Robotic Applications,” in *2023 IEEE 21st World Symposium on Applied Machine Intelligence and Informatics (SAMI)*, 2023, pp. 21–26. DOI: 10.1109/SAMI58000.2023.10044522 (cit. on p. 2).
- [25] K. Zhu and T. Zhang, “Deep reinforcement learning based mobile robot navigation: A review,” *Tsinghua*

*Science and Technology*, vol. 26, no. 5, pp. 674–691, 2021. DOI: 10.26599/TST.2021.9010012 (cit. on p. 3).

[26] S. Fujimoto, H. van Hoof, and D. Meger, “Addressing function approximation error in actor-critic methods,” 2018. arXiv: 1802.09477 [cs.AI] (cit. on p. 3).



**Seunghyeop Nam** is a undergraduate researcher of computer science in Konkuk University Seoul Korea. He is in Distributed Multimedia Systems Laboratory (DMS Lab) at Konkuk University since 2021. His interests of research are deep reinforcement learning, robotic mechatronics, sensor fusion, vision deep learning and path planning of mobile robot.



**Tuan Anh Nguyen** (Ph.D.'15, M.Sc.'10, B.Eng.'08) is an Academic Research Assistant Professor at Konkuk University's Aerospace Design-Airworthiness Institute in Seoul, South Korea. He is a member of IEEE, IEEE Computer, Robotics and Automation (IEEE RAS), Aerospace and Electronic Systems (IEEE AESS), and Reliability Societies. He earned his Ph.D. in Computer Science and Systems Engineering from Korea Aerospace University and his MSc and BEng in Mechatronics from Hanoi University of Science and Technology.

His research focuses on Dynamics and Control Theory, AI-based Digital Twin Systems, and Autonomous Intelligent Systems.



**Eunmi Choi** currently at Kookmin University, Korea, specializes in big data infrastructure, cloud computing, intelligent systems, information security, parallel and distributed systems, and software architecture. She earned her M.S. and Ph.D. in Computer Science from Michigan State University (1991, 1997) and her B.S. from Korea University (1988). Previously, she was an assistant professor at Handong University (1998-2004). She leads the Distributed Information System and Cloud Computing Lab at Kookmin University.



**Dugki Min** received a B.S. degree in industrial engineering from Korea University in 1986, an M.S. degree in 1991 and a Ph.D. degree in 1995, both in computer science from Michigan State University. He is currently a Professor in Department of Computer Science and Engineering at Konkuk University. His research interests include cloud computing, distributed and parallel processing, big data processing, intelligent processing, software architecture, and modelling and simulation.